Sharwes Scientific Journal (SSJ)
Volume 7, Issue 1, 2026, pp 201-217.
ISSN (Print): 3079-6040 • ISSN (Online): 3135-4343

Utilization of Dry Seaweed (DSWAC) for Removal of zinc ions (Zn^{2+}) from Aqueous Solution

Ali Hgeig[1], Gamal Ftes[2], Ezdehar Althallouti[3], Karima Ben yahya[3]

[1] Department of Civil Engineering, Faculty of Engineering, Jado, University of Nalut, Nalut Libya.
[2] Department of Farwa Marine Protected Area, Marine Biology Research Center, Tajora, Libya.
[3] Department of Marine Chemistry and Physics, Marine Biology Research Center, Tajora, Libya.

*Corresponding author: Ali Hgeig | ali.hgeig@nu.edu.ly

Received: 26-03-2026 | Accepted: 25-04-2026 | Available online: 07-05-2026 | DOI:10.5281/zenodo.20073665

ABSTRACT

Dry seaweed (DSWAC) was utilized as a precursor for the preparation of activated carbon through chemical activation using phosphoric acid at 400 °C. The activation process was carried out with different impregnation ratios of H_3PO_4 (H_3PO_4/ Dry seaweed): $3{:}1^{30\%}$, $4{:}1^{30\%}$, $3{:}1^{50\%}$, and $4{:}1^{50\%}$. The effects of several key operational parameters, including contact time, initial metal ion concentration, adsorbent dosage and pH. The equilibrium data were analyzed using the Langmuir, Freundlich, and Temkin adsorption isotherm models, the Langmuir and Freundlich showed satisfactory correlation coefficients. According to the Langmuir model, the maximum adsorption capacity was determined to be 58.90 mg g^{-1} at room temperature. The adsorption kinetics of zinc ions (Zn^{2+}) were evaluated using pseudo-first-order, pseudo-second-order, and intraparticle diffusion models. Among these models, the pseudo-second-order model provided the best description of the kinetic data. Overall, the (DSWAC) adsorbent demonstrated significant potential for zinc ions (Zn^{2+}) removal from aqueous solutions, highlighting its applicability as an environmentally friendly and low-cost adsorbent material.

Keywords: Dry seaweed, Activated carbon, zinc ions (Zn^{2+}), low-cost adsorbent.

استخدام الأعشاب البحرية الجافة (DSWAC) لإزالة أيونات الزنك (Zn^{2+}) من المحاليل المائية

علي حقيق[1*]، جمال فطيس[2]، إزدهار التلوثي[3]، كريمة بن يحي[3]

[1] قسم الهندسة المدنية ، كلية الهندسة_ جادو ، جامعة نالوت ، نالوت، ليبيا.
[2] قسم محمية فروة البحرية، مركز بحوث الاحياء البحرية ، تاجوراء، ليبيا.
[3] قسم الكيمياء والفيزياء مركز بحوث الاحياء البحرية، تاجوراء، ليبيا.

*المؤلف المراسل: علي حقيق | ali.hgeig@nu.edu.ly

استقبلت: 26-03-2026م | قبلت: 25-04-2026م | متوفرة على الانترنت | 07-05-2026م | DOI:10.5281/zenodo.20073665

ملخـــــص البحـــــث

تم استخدام الأعشاب البحرية الجافة (DSWAC) كمادة أولية لتحضير الكربون المنشّط من خلال التنشيط الكيميائي باستخدام حمض الفوسفوريك عند درجة حرارة 400 °م. وقد أُجريت عملية التنشيط باستخدام نسب تخصيب مختلفة من حمض الفوسفوريك (حمض الفوسفوريك/الاعشاب البحرية الجافة):1:3 $^{30\%}$, 1:4 $^{30\%}$, 1:3 $^{50\%}$, 1:4 $^{50\%}$, تمت دراسة تأثير عدد من المتغيرات الرئيسية، بما في ذلك زمن التلامس، والتركيز الابتدائي لأيونات المعدن، وجرعة المادة المدمصة، وقيمة الأس الهيدروجيني (pH). كما تم تحليل بيانات الاتزان باستخدام نماذج Langmuir، Freundlich، Temkin،

حيث أظهرت نماذج Langmuir و Freundlich معاملات ارتباط مرضية. وبحسب نموذج Langmuir ، تم تحديد السعة القصوى للامتزاز بقيمة 58.90 ملغم/غم عند درجة حرارة الغرفة. كما تم تقييم حركية امتزاز أيونات الزنك (Zn^{2+}) باستخدام نماذج الرتبة الأولى ، والرتبة الثانية ، ونموذج الانتشار داخل الجسيمات، حيث أظهر نموذج الرتبة الثانية أفضل توافق مع البيانات الحركية. وبشكل عام، أظهرت المادة المدمصة (DSWAC) قدرة عالية على إزالة أيونات الزنك (Zn^{2+}) من المحاليل المائية، مما يبرز إمكانية استخدامها كمادة مدمصة صديقة للبيئة ومنخفضة التكلفة.

الكلمات المفتاحية: الأعشاب البحرية الجافة؛ الكربون المنشط؛ أيونات الزنك؛ مدمص منخفض التكلفة.

1. Introduction

Water resources are among the most pressing environmental challenges globally Across the globe, environmental regulations governing the release of contaminants into natural ecosystems have become increasingly strict. Consequently, wastewater discharge into the environment is now subject to more rigorous control measures. Among the various pollutants of concern, heavy metals have attracted considerable attention because of their potential health risks, as they can be absorbed by living organisms and accumulate within biological systems. Their persistence in soils, sediments, and the food chain may ultimately lead to severe consequences for human health. A well-known example is the Minamata incident in Japan, where mercury accumulation in the food chain caused serious health impacts [1,2].

Although the removal of toxic heavy metals from industrial wastewater has been practiced for several decades, the efficiency—particularly the cost-effectiveness—of conventional physicochemical treatment methods remains limited. In this context, biological materials have emerged as promising alternatives for heavy metal removal; however, practical application requires biosorbents that are inexpensive and possess sufficiently high metal-binding capacity and selectivity toward heavy metals [3,4].

Zinc is an essential trace element required for biological functions; however, when present at concentrations exceeding permissible limits, it may cause adverse effects on human health. The World Health Organization (WHO) has established a provisional guideline value of 5 mg L^{-1} for zinc in drinking water. Zinc commonly occurs in inorganic forms, predominantly in the +2 oxidation state, and is widely used in industrial processes such as galvanization, pigment production, stabilizers, thermoplastics, alloy manufacturing, and battery production. During metallurgical and industrial operations, zinc may be released into aquatic environments. Due to their non-biodegradable nature and persistence, heavy metals can accumulate in soils, sediments, and the food chain, posing significant risks to human health [5,6].

Several techniques have been developed for metal ion removal from wastewater, including chemical precipitation, ion exchange, reverse osmosis, and adsorption. Chemical precipitation is widely applied; however, the generated sludge often contains high concentrations of heavy metals, creating disposal challenges. As a result, adsorption has gained significant attention due to its simplicity and effectiveness. Various natural materials such as zeolite, apatite, and bentonite, as well as industrial by-products including fly ash [7,8] , red mud, and blast furnace slag [9]. Activated carbon remains the most widely used adsorbent due to its high surface area and strong adsorption capacity [10].

Nevertheless, its relatively high cost restricts large-scale application, particularly in developing countries. Consequently, agricultural and forestry residues such as sawdust, rice husk, used tea leaves, straw, and seeds have been explored as alternative low-cost adsorbents [11,12,13].

In light of these considerations, the present study investigates the removal of Zn^{2+} ions from aqueous solutions using activated carbon prepared from dry seaweed (DSWAC). The adsorption performance of the synthesized adsorbent was evaluated to determine its potential as an efficient, low-cost, and environmentally friendly material for zinc removal from contaminated water

2. Materials and Methods

2.1. Sample preparation and analysis of inorganic pollutant

All chemicals used in this study were of analytical grade and supplied by Fluka. Zinc nitrate ($Zn(NO_3)_2$), concentrated hydrochloric acid (HCl), Sodium hydroxide NaOH, and phosphoric acid (H_3PO_4, 85%) were used without further purification. Stock solutions were prepared and diluted to the desired concentrations using deionized water produced by an EASYpure® II Reservoir Feed Water Purification System. The concentration of zinc ions (Zn^{2+}) in the supernatant was determined using a flame atomic absorption spectrometer (FAAS) (AM Series AA Spectrometer, England) equipped with an air–acetylene flame. The solution pH was measured using a pH meter (Violence XS, Italy). Drying of samples was carried out using a laboratory oven (Gallenkamp, BS Oven 250, Size 3, England), while carbonization was performed using a muffle furnace (Thermo Electron Corporation). Batch adsorption experiments were conducted using a mechanical shaker (Innova 4340, England).

2.2. Untreated lignocellulosic biomass

Seaweed is a naturally occurring marine biomass widely distributed along the Libyan Mediterranean coastline. In this study, the raw material was collected from the Farwa Marine Protected Area, located in the western coastal region of Libya. It consists of various species of marine macroalgae that are frequently washed ashore as a result of tidal activity and seasonal storms. Large quantities of this biomass accumulate along the coastline and are often removed as waste during routine beach cleaning operations. However, seaweed is rich in organic carbon and contains significant amounts of cellulose, hemicellulose, and lignin, making it a promising precursor for the production of activated carbon. Libya possesses an extensive Mediterranean coastline of more than 1,900 km, which leads to considerable seasonal accumulations of seaweed biomass. Although the exact quantities vary depending on environmental conditions, substantial amounts of this organic residue are generated annually, representing an abundant and renewable biomass resource.

2.3. Procedure of (DSWAC) adsorbent preparation

The collected seaweed was thoroughly washed with hot distilled water to remove impurities and adhering particles. The cleaned biomass was then dried in an oven (Memmert, Germany) at 60 °C for 24 h prior to activation. After drying, the material was sieved and chemically impregnated with phosphoric acid (H_3PO_4) solutions at concentrations of 10%, 20%, and 30%. Two impregnation ratios of phosphoric acid to dried biomass (H_3PO_4: Dry seaweed), namely 1:2 and 1:4 (w/w), were employed during the activation process. The impregnation ratio (X_p) was defined according to *Hgeig et al.* [14,15] as the weight ratio of phosphoric acid to the dried

biomass. The mixtures were maintained under impregnation conditions for 24 h to ensure adequate penetration of the activating agent. The activated carbons prepared under different conditions were designated according to acid concentration and impregnation ratio as DSWAC-10-2, DSWAC-10-4, DSWAC-20-2, DSWAC-20-4, DSWAC-30-2, and DSWAC-30-4, where the first number represents the phosphoric acid concentration (%) and the second number indicates the impregnation ratio, as shown in Table 1. After impregnation, the samples were repeatedly washed with boiled distilled water until the pH stabilized and the wash water became clear, followed by drying at 110 °C for 24 h. Carbonization was carried out in an oven at 400 °C with a heating rate of 10 °C min^{-1} for 45 min. The resulting activated carbon was subsequently crushed and sieved to obtain particle sizes ranging from 100 to 200 µm, making it suitable for use as an adsorbent. The yield of the activated carbon, which represents the efficiency of the production process, was calculated using Equation (1).

$$\text{Yield (\%)} = \frac{W_1}{W_0} \times 100 \quad (1)$$

The weight loss during the production process was calculated according to Equation (2):

$$\text{Weight loss (\%)} = \frac{W_0 - W_1}{W_0} \times 100 \quad (2)$$

where W_0 is the weight of the original dry seaweed, and W_1 is the weight of the resulting activated carbon (DSWAC).

Table 1. Preparation conditions of the activated carbon samples.

Sample	H_3PO_4 concentration (%)	Impregnation ratio (H_3PO_4 : seaweed)
DSWAC-10-2	10	1:2
DSWAC-10-4	10	1:4
DSWAC-20-2	20	1:2
DSWAC-20-4	20	1:4
DSWAC-30-2	30	1:2
DSWAC-30-4	30	1:4

2.4. Batch adsorption experiment

The influence of key experimental parameters, including solution pH (2.0–10.0), adsorbent dosage (2.0 –2.0 g L^{-1}), contact time (10–150 min) and initial metal ion concentration (5–100 mg L^{-1}), on metal ion removal was systematically investigated under batch conditions. The solution pH was adjusted using 0.1 mol L^{-1} HCl or 0.1 mol L^{-1} NaOH. In all experiments, a predetermined mass of (DSWAC-30-2) was added to 50 mL of metal ion solution in Erlenmeyer flasks. The mixtures were agitated at 200 rpm using a rotary shaker, and samples were withdrawn at specified time intervals for analysis. The adsorption capacity at equilibrium, q_e(mg g^{-1}), was calculated using the following Equations (3) [15]:

$$q_e = \frac{(C_0 - C_e)V}{m} \quad (3)$$

where $C_0$and C_e(mg L^{-1}) represent the initial and equilibrium concentrations of the metal ion, respectively; V(L) is the volume of the solution; and m(g) is the mass of activated carbon used. The percentage removal efficiency (R%) was determined according to Equation (4)[16]:

$$R\% = \frac{C_0 - C_e}{C_0} \times 100 \quad (4)`$$

To evaluate the accuracy of kinetic and isotherm models in describing the experimental data, statistical error analyses were performed using the root mean square error (RMSE) tests, defined as follows(5) [17]:

$$RMSE = \sqrt{\frac{1}{N-2}\sum_{i=1}^{N}(q_{e,meas} - q_{e,cal})^2} \quad (5)$$

where $q_{e,meas}$ is the experimentally measured adsorption capacity, $q_{e,cal}$ is the value predicted by the applied kinetic or isotherm model, and N the total number of data points. Lower RMSE values indicate a better agreement between experimental results and model predictions [17] .

2.5. Adsorption isotherms

The interaction between the selected ion metal and the adsorbent can be described using three widely applied adsorption isotherm models, namely Langmuir, Freundlich, and Temkin. These models are commonly used to characterize the adsorption process and to provide insight into the nature of the adsorbent surface and the adsorption mechanism [18,19, 20].

The Langmuir isotherm assumes monolayer adsorption onto a homogeneous surface with a finite number of identical active sites. The linear form of the Langmuir model Eq. (6) is expressed as :

$$\frac{C_e}{q_e} = \frac{1}{q_{max} K_L} + \frac{C_e}{q_{max}} \quad (6)$$

where *qe* (mg g^{-1}) is the amount of adsorbate adsorbed at equilibrium, *Ce* (mg L^{-1}) is the equilibrium concentration, *qmax* (mg g^{-1}) is the maximum monolayer adsorption capacity, and *KL* (L mg^{-1}) is the Langmuir equilibrium constant.

The essential characteristics of the Langmuir model can be further evaluated using the dimensionless separation factor (*RL*), defined as Eq. (7) :

$$R_L = \frac{1}{1 + K_L C_O} \quad (7)$$

where C_0 (mg L^{-1}) is the initial concentration.

The Freundlich isotherm describes adsorption on heterogeneous surfaces and assumes a non-uniform distribution of adsorption sites. Its logarithmic form Eq. (8) is given as:

$$logq_e = logK_f + \frac{1}{n} logC_e \quad (8)$$

where K_F is the Freundlich constant related to adsorption capacity, and n is the heterogeneity factor.

The Temkin isotherm considers adsorbate–adsorbent interactions and assumes that the heat of adsorption decreases linearly with increasing surface coverage. The Temkin model Eq. (9) is expressed as :

$$q_{e=} \frac{RT}{b} \ln A + \frac{RT}{b} \ln C_e \quad (9)$$

where A (L g^{-1}) is the Temkin equilibrium binding constant, b is related to the heat of adsorption (J mol^{-1}), R is the universal gas constant (8.314 J mol^{-1} K^{-1}), and T is the absolute temperature (K).

2.6. Adsorption kinetics

To investigate the adsorption mechanism of zinc ions (Zn^{2+}) onto (DSWAC-30-2) and to adequately describe the adsorption kinetics, three widely used kinetic models were applied, namely the pseudo-first-order, pseudo-second-order, and intraparticle diffusion models. The pseudo-first-order kinetic model Eq. (10) assumes that the rate of occupation of adsorption sites is proportional to the number of unoccupied sites. Its linear form is expressed as follows [21,22]:

$$\log(q_e - q_t) = \log q_e - \frac{k_1}{2.303} t \quad (10)$$

where q_e and q_t (mg g^{-1}) represent the adsorption capacities at equilibrium and at time t, respectively, and k_1 (min^{-1}) is the pseudo-first-order rate constant.

The pseudo-second-order kinetic model Eq. (11) assumes that the adsorption process is controlled by chemisorption. The linear form of this model is given by:

$$\frac{t}{q_t} = \frac{1}{k_2 q_e^2} + \frac{t}{q_e} \quad (11)$$

where k_2 (g mg^{-1} min^{-1}) is the pseudo-second-order rate constant.

The intraparticle diffusion model proposed by Weber–Morris Eq. (12) is expressed as:

$$q_t = k_{id}\, t^{\frac{1}{2}} + C_i \quad (12)$$

where k_id (mg g^{-1} $min^{-1/2}$) is the intraparticle diffusion rate constant, and C_i (mg g^{-1}) is a constant related to the thickness of the boundary layer.

3. Results and discussion

3.1. Parameters influencing adsorption

In this section, the influence of various operational parameters on the adsorption of the target metal ion onto (DSWAC-30-2) was systematically evaluated.

3.1.1. Impact of H_3PO_4 concentration

The prepared DSWAC demonstrated high efficiency for the removal of zinc ions (Zn^{2+}) from aqueous solutions, which can be attributed to its well-developed porous structure and enhanced surface functionality. Chemical activation using H_3PO_4 played a critical role in tailoring the physicochemical properties of the adsorbent by promoting dehydration reactions and facilitating crosslinking within the biomass matrix. During carbonization, H_3PO_4 effectively suppressed tar formation and reduced the volatilization of intermediate compounds, thereby enhancing char yield quality and pore development. The optimum preparation conditions were achieved at an impregnation ratio (H_3PO_4/dry seaweed) of 1:2 with an acid concentration of 30%, under which the adsorbent exhibited maximum zinc ions (Zn^{2+}) removal at pH 6.0. The relatively high weight loss (68.24%) observed during thermal treatment is attributed to the decomposition of volatile matter and the elimination of non-carbon species, which contributed to the formation of a highly porous carbon structure. Despite the moderate yield (31.76%), the developed adsorbent exhibited superior adsorption performance, indicating that pore formation and surface functionality are more critical than mass retention. Overall, the results highlight that H_3PO_4 activation is an effective strategy for producing high-performance adsorbents from seaweed biomass, offering a promising and sustainable approach for heavy metal removal from aqueous systems.

3.1.2. Effect of solution pH on adsorption

The solution pH plays a crucial role in controlling both the adsorption efficiency and mechanism of zinc ions (Zn^{2+}) removal. It influences zinc ions (Zn^{2+}) speciation in solution as well as the surface charge and ionization of functional groups on the adsorbent. The adsorption capacity of (DSWAC-30-2) was evaluated over a pH range of 2.0–10.0 under batch conditions (C_0 = 50 mg L^{-1}, adsorbent dosage = 16 g L^{-1}, contact time = 20 min, T = 25 ± 1 °C). The results revealed a strong dependence of zinc ions (Zn^{2+}) adsorption on solution pH. At low pH values, the adsorption capacity was significantly reduced due to the high concentration of H^+ ions, which compete with zinc ions (Zn^{2+}) for active sites. As the pH increased, deprotonation of surface functional groups enhanced the electrostatic attraction between the negatively charged

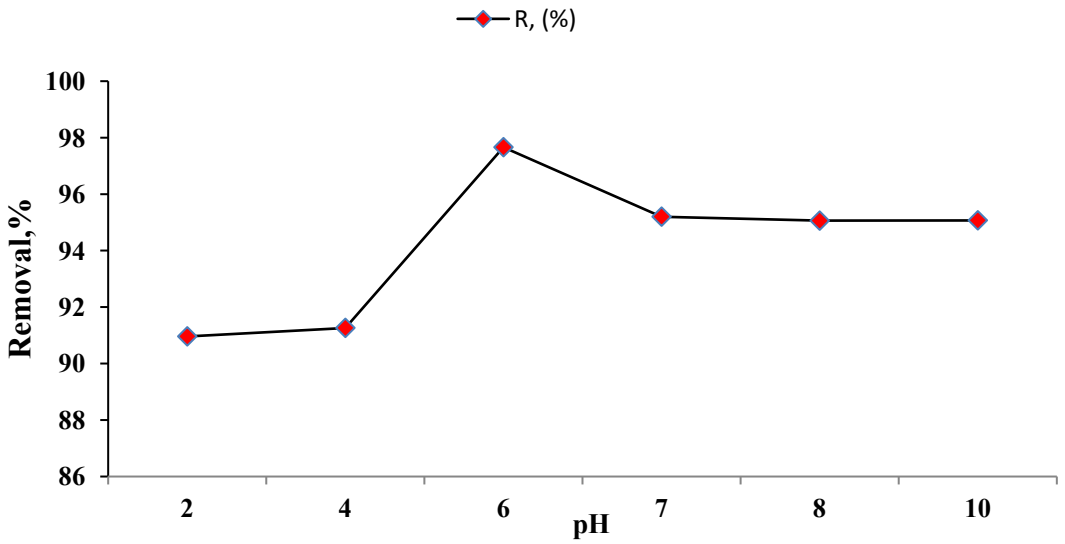

Fig 1. Effect of pH on adsorption of Zn on (DSWAC-30-2), C_o = 50.0 mg L^{-1}, Cont. time = 20 min,Mass of adsorbent 16 g L^{-1}).

adsorbent surface and zinc ions (Zn^{2+}), resulting in improved adsorption performance. The maximum removal efficiency 97.60% was achieved at pH 6.0 Fig .1. However, at pH values above 6.5, the formation of $Zn(OH)_2$ precipitates was observed, indicating that the decrease in dissolved zinc ions (Zn^{2+}) concentration cannot be attributed solely to adsorption. Therefore, pH 6.0 was selected as the optimal condition to ensure that zinc ions (Zn^{2+}) removal occurs predominantly via adsorption rather than precipitation. This behavior is consistent with previous studies, which reported that zinc ions (Zn^{2+}) adsorption is favored at near-neutral pH due to reduced proton competition and increased surface negativity of the adsorbent [23,24]

3.1.3. Effect of activated carbon dosage

The dosage of adsorbent plays a significant role in adsorption processes because it determines the available surface area and the number of active adsorption sites. To evaluate this effect, experiments were conducted using different masses of activated carbon ranging from 2.0 to 20 g L^{-1}. During these experiments, the operational conditions were maintained at an initial zinc ions (Zn^{2+}) concentration of 50 mg L^{-1}, a contact time of 30 min, a reaction temperature of 25 ± 1 °C, and a solution pH of 6.0. The results, illustrated in Fig. 2, indicate that increasing the activated carbon dosage resulted in a decrease in adsorption capacity. Specifically, the amount of zinc ions (Zn^{2+}) adsorbed declined from 196.25 mg g^{-1} at 2.0 g L^{-1} to 30.38 mg g^{-1} at 16 g L^{-1} of adsorbent. In contrast, the removal efficiency increased from 78.50% to 97.20% with increasing adsorbent dosage, due to the greater availability of adsorption sites for zinc ions (Zn^{2+}). This behavior can be attributed to the increased number of available adsorption sites relative to the fixed concentration of metal ions in the solution, which leads to a lower amount of adsorbed ions per unit mass of adsorbent. Furthermore, increasing the adsorbent dosage beyond 16 g L^{-1} did not lead to a significant improvement in the removal efficiency. Considering both adsorption performance and operational cost efficiency, an activated carbon dosage of 16 g L^{-1} was therefore selected as the optimal value for subsequent batch adsorption experiments and for potential applications in the treatment of metal-contaminated water.

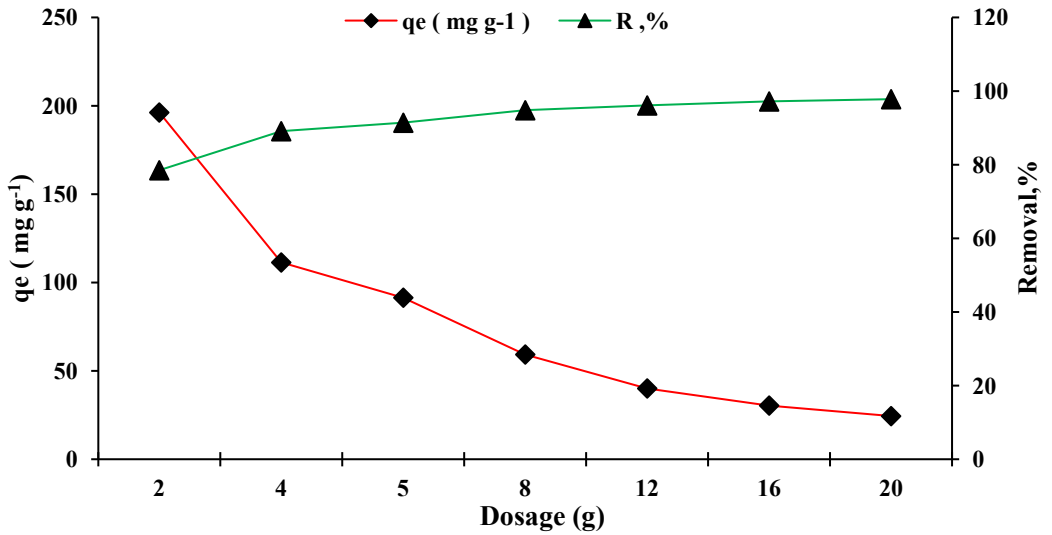

Fig.2. Influence of DSWAC-30-2 dosage on the Zn^{2+} adsorption process (C_0 =50 mg L^{-1}, Cont. time = 30 min, pH = 6.0)

.3.1.4. Effect of contact time

The influence of contact time on the adsorption of zinc ions (Zn^{2+}) from aqueous solutions using (DSWAC-30-2) was investigated under batch conditions at different time intervals (10, 20, 30, 40, 60, 90, and 120 min). The experiments were conducted at an initial Zn^{2+} concentration of 50 mg L^{-1}, at the optimal pH of 6.0 and room temperature (25 ± 1 °C). The adsorbent dosage was maintained at 0.8 g (16 g L^{-1}) in 50 mL of solution. As illustrated in Fig. 3, (DSWAC-30-2) exhibited a strong affinity toward zinc ions (Zn^{2+}), resulting in rapid adsorption during the initial stage of contact. A significant increase in adsorption capacity was observed within the first 20 min, reaching 30.50 mg g^{-1} with a removal efficiency of approximately 97.50%. This rapid uptake can be attributed to the abundance of available active sites on the adsorbent surface and the high concentration gradient between zinc ions (Zn^{2+}) in the solution and the (DSWAC-30-2) surface. Beyond this period, no noticeable increase in adsorption capacity was observed with further increases in contact time, indicating that most of the available adsorption sites had been occupied and that adsorption equilibrium had been achieved. Similar rapid adsorption behavior has been reported in previous studies on the removal of metal ions using various adsorbents [23,25]. Therefore, a contact time of 20 min was considered sufficient to reach equilibrium and was selected as the optimum contact time for subsequent adsorption experiments.

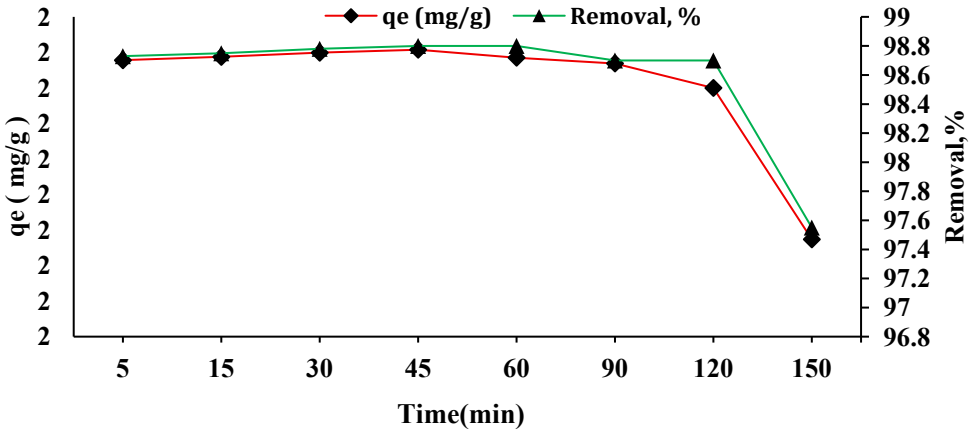

Fig.3. Influence of contact time for Zn^{2+} adsorption onto ((DSWAC-30-2) (C_0 = 50 mg L^{-1}, Mass of adsorbent 16 g L^{-1}, pH=6.0)

3.1.5. Effect of initial adsorbate concentration

The effect of the initial concentration of metal ion on the adsorption process was investigated at concentrations of 5, 10, 20, 30, 40, 50, 75, and 100 mg L^{-1}, while maintaining all other experimental conditions at their optimum levels: temperature of 25.0 ± 1 °C, pH 6.0, biochar dosage of 16 g L^{-1}, and a contact time of 20 min. The results indicated that the adsorption capacity increased with increasing initial metal ion concentration Fig. 4. This trend can be attributed to the higher ratio of the initial number of moles of zinc ions (Zn^{2+}) to the available adsorption sites at elevated concentrations [26]. Accordingly, the adsorption capacity of (DSWAC-30-2) increased from 3.12 to 58.90 mg g^{-1} as the initial metal ion concentration increased from 5 to 100 mg L^{-1}. However, at higher initial concentrations, the number of

available adsorption sites on (DSWAC-30-2) becomes relatively limited, leading to a decrease in the percentage removal of metal ions.

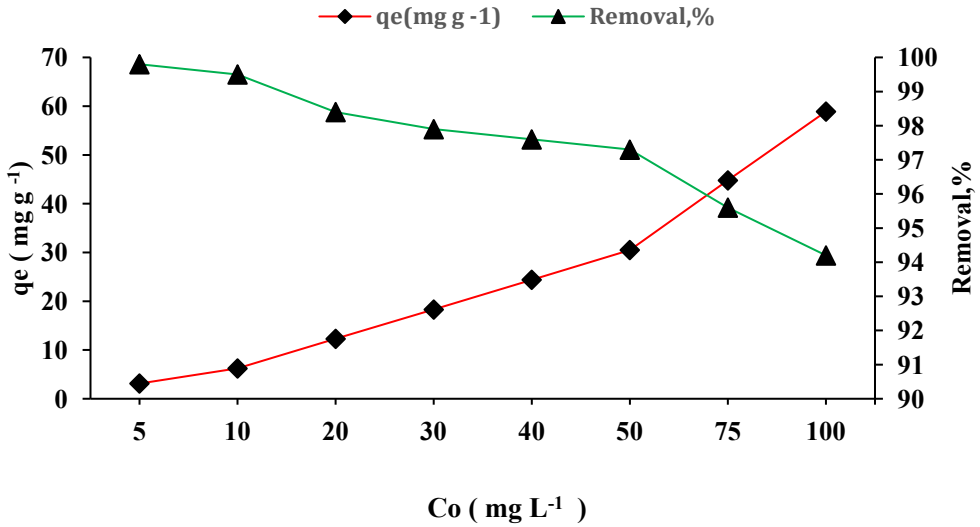

Fig. 4. Influence of the Zn^{2+} Concentration in the adsorption process Cont. time = 20. min, Mass of adsorbent 16 g L^{-1}, pH= 6.0)

3.2. Modeling of adsorption isotherms

The calculated isotherm parameters, correlation coefficients (R^2), and error functions (*RMSE*) are summarized in Table 2, while the graphical representations of the applied models are illustrated in Figs. 5 a, b ,c. The results indicate that the equilibrium adsorption data for zinc ions (Zn^{2+}) were well described by both the Langmuir and Freundlich isotherm models. The highest values of the correlation coefficient (R^2), together with the lowest *RMSE* values, were obtained for these models, indicating their suitability for describing the adsorption process. The Langmuir isotherm assumes monolayer adsorption on a homogeneous adsorbent surface with a finite number of identical active sites. According to this model, a significant adsorption capacity for zinc ions (Zn^{2+}) onto (DSWAC-30-2) was obtained, with a maximum monolayer adsorption capacity (q_{max}) of 58.90 mg g^{-1}. The favorability of the adsorption process was further evaluated using the dimensionless separation factor (R_L) derived from the Langmuir isotherm. The (R_L) values calculated for different initial concentrations of zinc ions (Zn^{2+}) are presented in Table 3. The obtained (R_L) values ranged from 0.003 to 0.062, which fall within the range of $0 < R_L < 1$, indicating favorable adsorption (Table 3). Moreover, R_L values decreased with increasing initial Zn^{2+} concentration, suggesting that the adsorption process becomes more favorable at higher metal ion concentrations. The very low (R_L) values observed at higher concentrations indicate a strong affinity between zinc ions (Zn^{2+}) and the (DSWAC-30-2) surface, further supporting the applicability of the Langmuir model and the assumption of monolayer adsorption.

Table 2. Isotherm constants of the Langmuir, Freundlich and Temkin models for Zn^{2+} uptake by (DSWAC-30-2)

	Isotherm model	Parameters
$q_{max,exp}$ (mg g^{-1})		65.789
Langmuir	q_{max} (mg g^{-1})	58.90
	K_L (L mg^{-1})	57.803
	r	0.955
	RMSE	0.652
Freundlich	K_f	24.80
	1/n	0.451
	r *RMSE*	0.993 1.730
Temkin	*B* (J L^{-1})	7.805
	A	52.40
	r *RMSE*	0.886 7.422

The Freundlich model, which describes adsorption on heterogeneous surfaces, also showed good agreement with the experimental data. The Freundlich constant (K_f), which reflects the adsorption capacity of the adsorbent, followed the same trend observed for the Langmuir constant (K_L) (Table 2). Furthermore, the values of the Freundlich parameter (*1/n*) satisfied the condition for favorable adsorption ($0 < 1/n < 1$), indicating that the adsorption of zinc ions (Zn^{2+}) onto (DSWAC-30-2) occurs under favorable conditions. The applicability of the Freundlich model suggests that the surface of (DSWAC-30-2) is heterogeneous and composed of adsorption sites with different energies. In contrast, the Temkin isotherm showed lower correlation coefficients (R^2) and higher *(RMSE)* values compared with the other models, indicating that this model does not adequately describe the adsorption behavior of Zn^{2+} ions onto (DSWAC-30-2) under the investigated conditions.

Table 3. The R_L values for (DSWAC-30-2)

C_o (mg L^{-1})	R_L
	Zn^{2+}
5	0.062
10	0.032
20	0.016
30	0.011
40	0.008
50	0.007
75	0.004
100	0.003

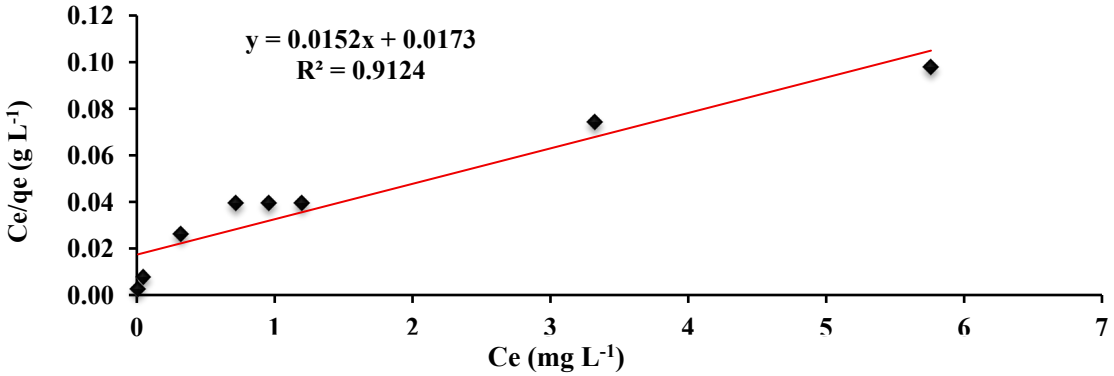

Fig. 5a. The linearized Langmuir isotherm of Zn^{2+} onto (DSWAC-30-2)

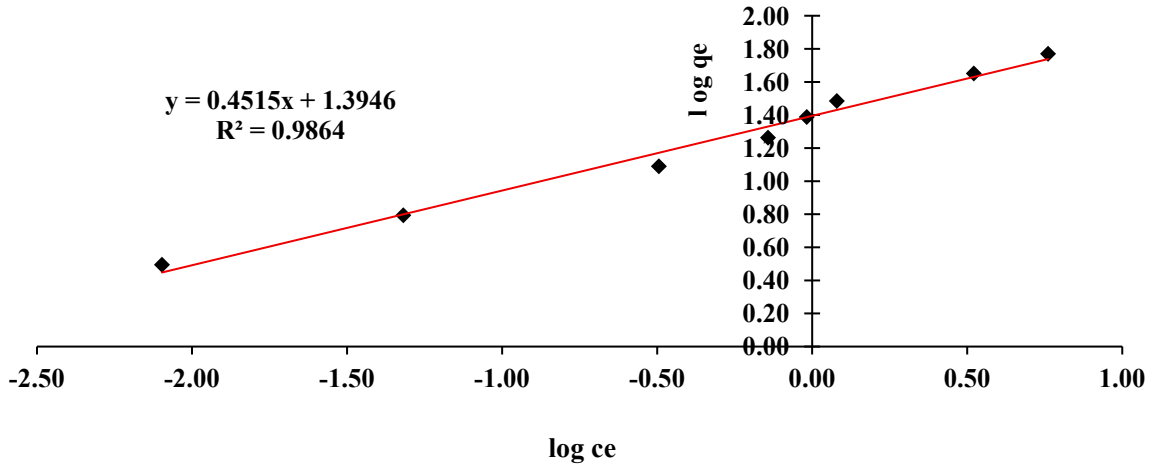

Fig. 5b. The linearized Freundlich isotherm of Zn^{2+} ions onto (DSWAC-30-2)

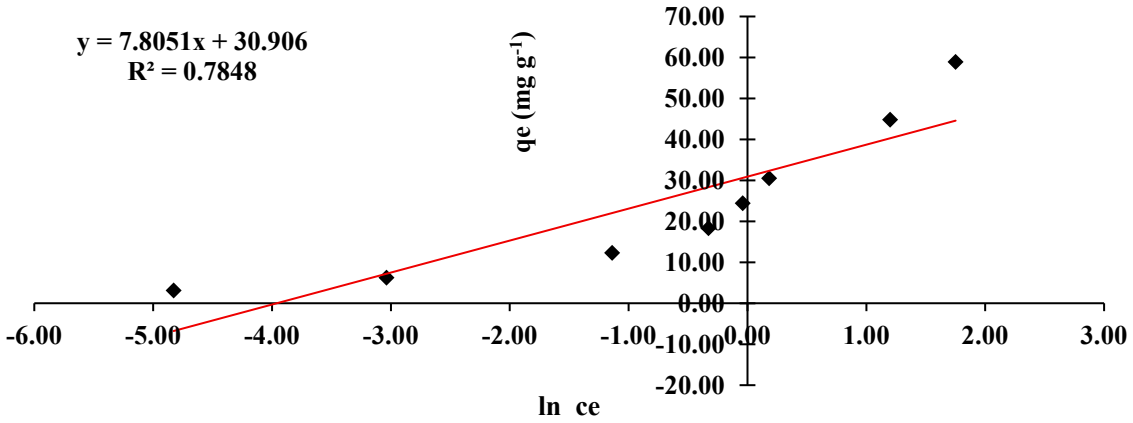

Fig. 5c. The linearized Temkin isotherm of Zn^{2+} ions onto (DSWAC-30-2)

3.3. Adsorption kinetics

All kinetic parameters obtained from the applied models, along with the corresponding correlation coefficients (R^2) and error functions, are summarized in Table 4, while the graphical representations of the kinetic models for the adsorption of zinc ions (Zn^{2+}) are presented in Figs. 6a, b, c. Among the investigated models, the pseudo-second-order kinetic model exhibited the highest R^2 values for all experimental kinetic data. In addition, the *RMSE* values associated with this model were the lowest compared with those obtained from the other kinetic models. These findings indicate that the adsorption of zinc ions (Zn^{2+}) onto (DSWAC-30-2) follows a pseudo-second-order kinetic mechanism. This suggests that the rate of adsorption is largely governed by the interaction between the metal ions and the active sites of the adsorbent surface and that the overall process is mainly controlled by chemisorption. Furthermore, the results presented in Table 4. demonstrate that the pseudo-first-order kinetic model and the intraparticle diffusion model are not suitable for describing the adsorption behavior of zinc ions (Zn^{2+}) onto (DSWAC-30-2). This limitation can be attributed to the negative slopes obtained for the pseudo-first-order kinetic model as well as the relatively low correlation coefficients *(R^2)* observed for both models [27].

Table 4. Kinetic parameters for the adsorption of zinc ions (Zn^{2+}) onto (DSWAC-30-2)

		Zn^{2+}
***q_e, exp* (mg g^{-1})**		36.00
Pseudo-first order	q_e (mg g^{-1})	6.753
	K_1 (min^{-1})	0.0016
	r	0.487
Pseudo-second order	$q_{e\,(}$ mg g^{-1})	30.675
	$K_{2\,(}$g $mg^{-1}.min^{-1}$)	0.180
	r	0.999
Intraparticle diffusion of (DSWAC-30-2)	K_i (mg g^{-1} $min^{-1/2}$)	0.1427
	C_i (mg g^{-1})	29.307
	r	0.539

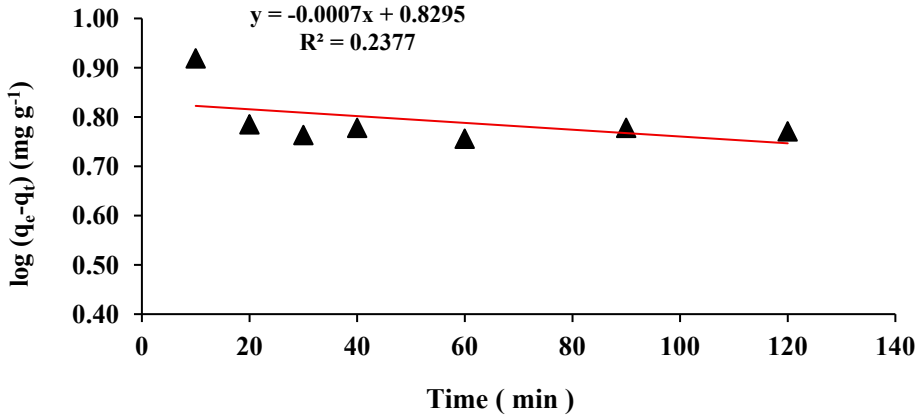

Fig. 6a. Pseudo-first order kinetics plot of Zn^{2+} onto (DSWAC_30_2)

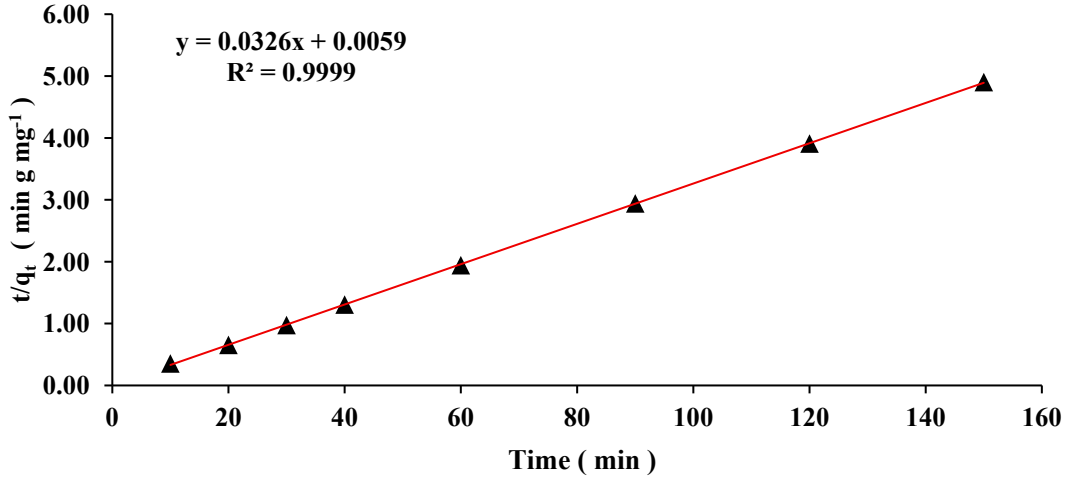

Fig. 6b. Pseudo-second order kinetics plot of Zn^{2+} onto (DSWAC_30_2)

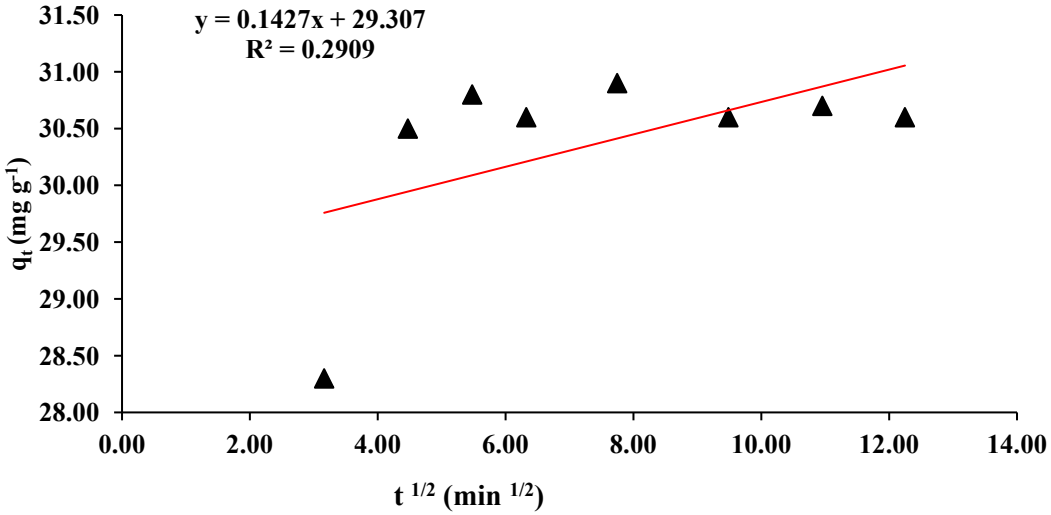

Figure 6c. Intraparticle diffusion plot of Zn^{2+} onto (DSWAC_30_2)

4. Discussion

The adsorption performance of (DSWAC-30-2) toward zinc ions (Zn^{2+}) demonstrates a strong dependence on both preparation conditions and operational parameters, indicating that the adsorption mechanism is governed by a combination of surface chemistry and mass transfer phenomena. The superior performance observed at an H_3PO_4 impregnation ratio of 1:2 and acid concentration of 30% suggests that chemical activation played a critical role in generating an optimal balance between pore development and functional group formation. This indicates that adsorption efficiency is more closely related to the availability of active sites than to the overall carbon yield. The effect of solution pH confirms that electrostatic interactions are a dominant factor in the adsorption process. At low pH values, competition between H^+ ions and Zn^{2+} ions reduces adsorption efficiency, whereas at near-neutral pH, deprotonation of functional groups enhances metal uptake. The observed optimum at pH 6.0 further indicates that adsorption occurs primarily through surface interaction mechanisms rather than precipitation, which becomes significant at higher pH levels. The inverse relationship between adsorption capacity (q_e) and adsorbent dosage reflects a typical adsorption behavior where an excess of available active sites leads to underutilization of the adsorbent surface. This suggests that adsorption is not only controlled by the number of active sites but also by the concentration gradient and effective collision between adsorbate and adsorbent particles. The rapid adsorption observed within the first 20 minutes indicates that external surface adsorption is the dominant mechanism during the initial stage, followed by a plateau phase corresponding to equilibrium conditions. This behavior is consistent with a fast interaction between zinc ions (Zn^{2+}) and the active functional groups on the adsorbent surface. The isotherm analysis reveals that both Langmuir and Freundlich models adequately describe the adsorption process, suggesting that the surface of (DSWAC-30-2) possesses both homogeneous and heterogeneous characteristics. The high adsorption capacity obtained from the Langmuir model (q_{max} = 58.90 mg g^{-1}) indicates strong affinity between zinc ions and the adsorbent surface, while the Freundlich model reflects the presence of sites with varying adsorption energies. Furthermore, the dominance of the pseudo-second-order kinetic model suggests that chemisorption is the rate-controlling mechanism, involving electron sharing or exchange between zinc ions and functional groups on the adsorbent surface. The poor fitting of the pseudo-first-order and intraparticle diffusion models indicates that physical adsorption and internal diffusion are not the primary controlling mechanisms under the studied conditions. Overall, the adsorption of zinc ions (Zn^{2+}) onto (DSWAC-30-2) can be described as a chemically controlled process influenced by surface functionality, solution chemistry, and operational parameters, highlighting the effectiveness of chemically activated seaweed as a viable adsorbent for heavy metal removal.

5. CONCLUSION

This study confirmed that activated carbon derived from dry seaweed (DSWAC) is an effective and sustainable adsorbent for the removal of zinc ions (Zn^{2+}) from aqueous solutions. The adsorption performance was strongly influenced by operational parameters, with optimum conditions achieved at pH 6.0, 16 g L^{-1} adsorbent dosage, and 20 min contact time, resulting in high removal efficiency and adsorption capacity. Equilibrium data were well described by both Langmuir and Freundlich isotherm models, indicating favorable adsorption behavior with both homogeneous and heterogeneous surface characteristics. The maximum adsorption capacity

(58.90 mg g^{-1}) reflects a strong affinity between zinc ions (Zn^{2+}) and the adsorbent surface. Kinetic analysis showed that the adsorption process follows a pseudo-second-order model, suggesting that chemisorption is the dominant mechanism. These findings demonstrate that DSWAC represents a promising low-cost and environmentally friendly material for zinc removal from contaminated water. However, further studies are recommended to evaluate its performance in complex systems and to assess its practical applicability at larger scales.

Acknowledgment

The authors would like to express their sincere appreciation to the Marine Biology Research Center, Tajura, Libya, for providing laboratory facilities and technical support.

References

[1] Ishneebeesh A, Alahrash S, Alakhdar A. Experimental study on electromagnetic treatment for reducing salinity in groundwater. J Multidiscip Eng. 2026;1:21-30.

[2] K. H. Hama Aziz, F. S. Mustafa, K. M. Omer, S. Hama, R. F. Hamarawf, and K. O. Rahman, "Heavy metal pollution in the aquatic environment: efficient and low-cost removal approaches to eliminate their toxicity: a review. RSC Adv 13: 17595–17610," 2023. DOI: 10.1039/D3RA00723E

[3] S. A. Razzak *et al.*, "A comprehensive review on conventional and biological-driven heavy metals removal from industrial wastewater," *Environmental Advances*, vol. 7, p. 100168, 2022. https://doi.org/10.1016/j.envadv.2022.100168

[4] S. A. Gouda and A. Taha, "Biosorption of heavy metals as a new alternative method for wastewater treatment: a review," *Egyptian Journal of Aquatic Biology and Fisheries*, vol. 27, no. 2, pp. 135–153, 2023.DOI: 10.21608/ejabf.2023.291671

[5] G. S. Murugesan, M. Sathishkumar, and K. Swaminathan, "Arsenic removal from groundwater by pretreated waste tea fungal biomass," *Bioresource Technology*, vol. 97, no. 3, pp. 483–487, 2006. https://doi.org/10.1016/j.biortech.2005.03.008

[6] M. Kobya, E. Demirbas, E. Senturk, and M. Ince, "Adsorption of heavy metal ions from aqueous solutions by activated carbon prepared from apricot stone," *Bioresource technology*, vol. 96, no. 13, pp. 1518–1521, 2005. https://doi.org/10.1016/j.biortech.2004.12.005

[7] S. I. Shofia, A. S. Vickram, A. Saravanan, V. C. Deivayanai, and P. R. Yaashikaa, "Sustainable separation technologies for heavy metal removal from wastewater: An upgraded review of physicochemical methods and its advancements," *Sustainable Chemistry for the Environment*, vol. 10, p. 100264, 2025. https://doi.org/10.1016/j.scenv.2025.100264

[8] Z. Li, G. Lu, D. Du, and D. Zhao, "Harnessing low-cost adsorbents for removal of heavy metals and metalloids in contaminated water: Progress in the past decade and future perspectives," *Journal of Cleaner Production*, vol. 518, p. 145845, 2025. https://doi.org/10.1016/j.jclepro.2025.145845

[9] W. Duan, X. Dong, Z. Wang, J. Yang, and B. Li, "Efficient adsorbent preparation from blast furnace slag: study on CO2 adsorption/desorption mechanism of layered double oxides," *Journal of Environmental Chemical Engineering*, p. 120679, 2025. https://doi.org/10.1016/j.jece.2025.120679

[10] H. Deng, T. Li, H. Li, A. Dang, and Y. Han, "Amine-modified graphene oxide: Reaction mechanism with functional groups and enhanced CO2 adsorption-separation performance," *Journal of Solid State Chemistry*, p. 125617, 2025. https://doi.org/10.1016/j.jssc.2025.125617

[11] M. Akhtar, M. Sarfraz, M. Ahmad, N. Raza, and L. Zhang, "Use of low-cost adsorbent for waste water treatment: Recent progress, new trend and future perspectives," *Desalination and Water Treatment*, vol. 321, p. 100914, 2025. https://doi.org/10.1016/j.dwt.2024.100914

[12] L. A. Torres-Castañón, A. Robledo-Peralta, C. Antileo, F. de J. Silerio-Vázquez, and J. B. Proal-Nájera, "Sawdust-based adsorbents for water treatment: An assessment of their potential and challenges in heavy metal adsorption," *Journal of Hazardous Materials Advances*, vol. 18, p. 100758, 2025. https://doi.org/10.1016/j.hazadv.2025.100758

[13] K. Das *et al.*, "Transformative and sustainable insights of agricultural waste-based adsorbents for water defluoridation: Biosorption dynamics, economic viability, and spent adsorbent management," *Heliyon*, vol. 10, no. 8, 2024. DOI10.1016/j.heliyon.2024.e29747

[14] A. Hgeig, M. Novaković, and I. Mihajlović, "Sorption of carbendazim and linuron from aqueous solutions with activated carbon produced from spent coffee grounds: Equilibrium, kinetic and thermodynamic approach," *Journal of Environmental Science and Health, Part B*, vol. 54, no. 4, pp. 226–236, 2019. https://doi.org./10.1080/03601234.2018.1550307

[15] I. Mihajlović *et al.*, "Valorizing date seeds into biochar for pesticide removal: a sustainable approach to

agro-waste-based wastewater treatment," *Sustainability*, vol. 17, no. 11, p. 5129, 2025. https://doi.org/10.3390/su17115129

[16] S. Pap, L. Shearer, and S. W. Gibb, "Effective removal of metformin from water using an iron-biochar composite: Mechanistic studies and performance optimisation," *Journal of Environmental Chemical Engineering*, vol. 11, no. 5, p. 110360, 2023. https://doi.org/10.1016/j.jece.2023.110360

[17] A. Hgeig, "Utilization of exhausted coffee waste and date stones for removal of pesticides from aquatic media," 2020, *University of Novi Sad (Serbia)*.

[18] X. Xing, N. S. Alharbi, X. Ren, and C. Chen, "A comprehensive review on emerging natural and tailored materials for chromium-contaminated water treatment and environmental remediation," *Journal of Environmental Chemical Engineering*, vol. 10, no. 2, p. 107325, 2022. https://doi.org/10.1016/j.jece.2022.107325

[19] S. Kanwal, P. Devi, Z. Ahmed, and N. A. Qambrani, "Adsorption isotherm, kinetic and thermodynamic studies for adsorption of fluoride on waste marble powder," *Desalination and Water Treatment*, vol. 319, p. 100441, 2024. https://doi.org/10.1016/j.dwt.2024.100441

[20] A. Mudhoo, "Unveiling new insights: Revised Temkin adsorption isotherm parameters from fresh curve fits in adsorption studies," *Chemical Engineering Science*, vol. 311, p. 121585, 2025. https://doi.org/10.1016/j.ces.2025.121585

[21] M. M. H. Rocky *et al.*, "Modeling sorption kinetics in environmental separations: Advancing beyond traditional pseudo-order approaches," *Separation and Purification Technology*, vol. 383, p. 135987, 2026. https://doi.org/10.1016/j.seppur.2025.135987

[22] H. Zhang, W. Zhong, R. Qiu, and L. Han, "Kinetics and modeling of Pb (II) adsorption in pellet biochar based on micro-computed tomography characterization," *Bioresource Technology*, vol. 387, p. 129645, 2023. https://doi.org/10.1016/j.biortech.2023.129645

[23] S. Pap, T. Š. Knudsen, J. Radonić, S. Maletić, S. M. Igić, and M. T. Sekulić, "Utilization of fruit processing industry waste as green activated carbon for the treatment of heavy metals and chlorophenols contaminated water," *Journal of Cleaner Production*, vol. 162, pp. 958–972, 2017. https://doi.org/10.1016/j.jclepro.2017.06.083

[24] P. C. Mishra and R. K. Patel, "Removal of lead and zinc ions from water by low cost adsorbents," *Journal of hazardous materials*, vol. 168, no. 1, pp. 319–325, 2009. https://doi.org/10.1016/j.jhazmat.2009.02.026

[25] S. Pap *et al.*, "Evaluation of the adsorption potential of eco-friendly activated carbon prepared from cherry kernels for the removal of Pb2+, Cd2+ and Ni2+ from aqueous wastes," *Journal of Environmental Management*, vol. 184, pp. 297–306, 2016. https://doi.org/10.1016/j.jenvman.2016.09.089

[26] H. Lalhruaitluanga, K. Jayaram, M. N. V Prasad, and K. K. Kumar, "Lead (II) adsorption from aqueous solutions by raw and activated charcoals of Melocanna baccifera Roxburgh (bamboo)—a comparative study," *Journal of hazardous materials*, vol. 175, no. 1–3, pp. 311–318, 2010. DOI: 10.1039/D3RA00723E

[27] M. Elazabi, B. Draskovic, M. Novakovic, I. Mihajlovic, and A. Hgeig, "Adsorption of Linuron and Isoproturon Pesticides on Commercial Activated Carbon, Norit SA2," Fresenius Environ. Bull, vol. 30, pp. 1030–1043, 2021.